JOURNAL OF THERMOPHYSICS AND HEAT TRANSFER
Vol. 12, No. 4, October–December 1998

Measured Shock-Layer Vibrational Populations and Temperatures in Arcjet Nitrogen Flow

Harvel E. Blackwell*
BSA Services, Houston, Texas 77045
Carl D. Scott†
NASA Johnson Space Center, Houston, Texas 77058
and
Sivaram Arepalli‡
G. B. Tech/Lockheed Martin, Houston, Texas 77058

Radiation is analyzed from a highly nonequilibrium shock layer produced by a blunt body in a low-density arcjet flow of nitrogen. Populations of vibrational states are obtained at several locations in the shock layer through fits of basis spectra to measured spectra. Several techniques determine the rotational and vibrational temperature corresponding to Boltzmann fits to low vibrational state populations for N_2 and N_2^+ molecules. These techniques include correlations of ratios of intensity integrals, fits of calculated vibrational basis sets to measurements, and minimization of the deviation between calculated and measured spectra. Analyses of basis set fits yield vibrational populations that deviate from a Boltzmann distribution at vibrational quantum numbers greater than about 6–8. Differences in rotational and vibrational temperatures are found, together with temperature differences between the neutral molecule and the ion. Temperature profiles and non-Boltzmann vibrational populations indicate the nonequilibrium character of the layer. Experimentally determined population distributions should interest anyone modeling nonequilibrium vibrational kinetics. These distributions, up to $v' = 20$, should be of interest, and temperature profiles generally should be useful when validating the gas models used for high-enthalpy nonequilibrium nitrogen flows.

Nomenclature

$A^2\Pi_u$ = electronic state of molecular nitrogen ion
$A^3\Sigma_u^+$ = electronic state of molecular nitrogen
$B^3\Pi_g$ = electronic state of molecular nitrogen
$B^2\Sigma_u^+$ = electronic state of molecular nitrogen ion
T_r = rotational temperature
T_v = vibrational temperature
v' = vibrational quantum number of upper state
v'' = vibrational quantum number of lower state
$X^1\Sigma_g^+$ = electronic ground state of molecular nitrogen
$X^2\Sigma_g^+$ = electronic ground state of molecular nitrogen ion

Introduction

LOCAL flow near a spacecraft during re-entry may be simulated by heating a gas in arcjets to enthalpies corresponding to flight velocities. A high-enthalpy flow is necessary to obtain the correct steady heat flux to test materials designed for spacecraft re-entry. It is difficult to simulate the enthalpy, pressure, and heat-flux parameters simultaneously in any ground facility. Often only the heat flux and pressure or the heat flux and enthalpy are simulated simultaneously. Flow in arcjets and flight is usually in thermochemical nonequilibrium, requiring knowledge of flow chemistry to determine surface chemical reactions such as catalytic recombination, surface oxidation, or even possible atomic nitrogen reactions with the surface. A careful analysis of the radiation spectrum from the shock layer of blunt bodies in arcjet flow can yield information that may be used to validate gas kinetic and radiation models developed to predict nonequilibrium flow in both test facilities as well as in flight. Before these measurements were undertaken, there was only one ground-based shock-layer measurement, a shock-tube measurement in 1963[1] used for model comparison. While, because of their continuous operation, arcjet flows present a more convenient means of shock-layer study, it is clear there are differences between arcjet shock layers and those found in shock tubes and flight. The manner in which shock-layer flow deviates from thermal equilibrium is significant in any case, and may be assessed with suitable spectroscopic measurements and analysis techniques.

Various emission spectroscopic techniques[2–9] have been used to determine temperatures and vibrational population distributions for N_2 and N_2^+ molecules. These techniques include fitting the measured spectra to sets of basis spectra corresponding to each vibrational level; integral ratio techniques; and one technique that separates P and R branches using an allocation scheme based on theory. Each of these methods is detailed in Ref. 10.

Measurements

Facility

Measurements were obtained at NASA Johnson Space Center in the flow of a constricted arc heater. This heater, which is powered by a 10-MW dc power supply, heats to high-enthalpy nitrogen or a mixture of nitrogen and oxygen to simulate air. The heated gas flows through a small settling chamber, then through a converging/diverging conical nozzle with a 5.71-cm-diam throat. The 38.1-cm nozzle exit in these exper-

Presented as Paper 97-2522 at the AIAA 32nd Thermophysics Conference, Atlanta, GA, June 23–25, 1997; received Sept. 12, 1997; revision received March 16, 1998; accepted for publication March 18, 1998.

*Chief Scientist. E-mail: heblack@wt.net. Member AIAA.
†Research Engineer, ES3, Structures and Mechanics Division. E-mail: c.scott@jsc.nasa.gov. Associate Fellow AIAA.
‡Senior Scientist, C61, Structures and Mechanics Division, P.O. Box 58561. E-mail: s.arepall@jsc.nasa.gov. Senior Member AIAA.

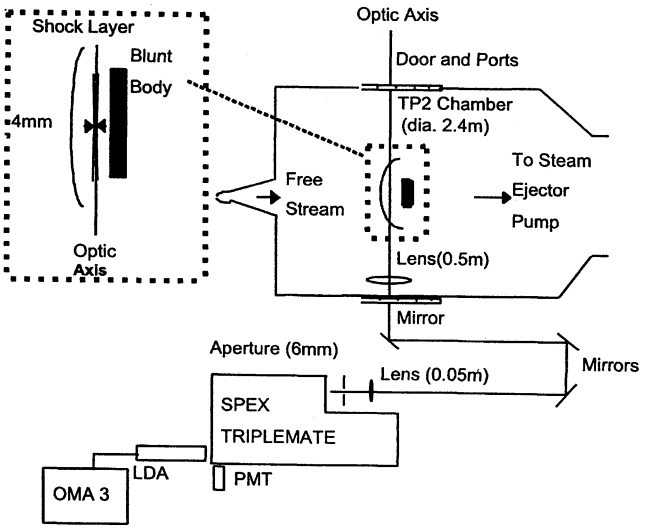

Fig. 1 Layout of spectral measurement apparatus with an inset showing the volume of acceptance of shock-layer radiation by the optical system.

iments was about 60 cm from the throat. Flow expands outside the nozzle into the test chamber containing a shock-forming body. The apparatus layout is given in Fig. 1.

Blunt Body

A water-cooled blunt body was inserted into the arcjet flow, where it produced a normal shock wave. The blunt body presented a 22.9 × 10.2-cm rectangular cross section to the flow. Its surface is a cylinder segment with a 25-cm radius that assures the stagnation line is well known. The rectangular body is quasi-two-dimensional, which minimizes the three-dimensional effects and lets us avoid a number of measurements that would normally be required to obtain an Abel inversion. However, because of the nonuniform flowfield, there was still some minor nonuniformity in the zone of spectral measurements.

Flow Conditions

Flow conditions for these measurements are an arc current of 600 A; a nitrogen gas flow rate of 54.4 g/s; and a bulk enthalpy, based on energy balance measurements, of 8.72 MJ/kg. The centerline enthalpy is estimated to be about a factor of 2 times the bulk enthalpy.[11] The blunt body was located on the centerline of the flow 14.3–16.5 cm from the nozzle exit. Shock-layer conditions are not expected to vary significantly over this small range of distances, however. The measured stagnation point pressure for these conditions (shown next) is approximately 1300 Pa. Estimated flow properties based on calculations for a centerline enthalpy of 17.4 MJ/kg: 1) Freestream = temperature 840 K, velocity 4000 m/s, density 3.1×10^{-3} kg/m^3, Mach numbber 5.9, pressure 30 Pa, mole fraction 0.406 N, and mole fraction 0.594 N_2. 2) Stagnation point = temperature 6500 K and calculated pressure 1400 Pa. Estimates of freestream and shock-layer flow conditions were calculated using the NATA code.[12] The NATA code solves one-dimensional (stream tube) inviscid flow equations for a chemically nonequilibrium, high-enthalpy gas through a variable-area nozzle, which accounts for nozzle wall boundary-layer displacement effects using boundary-layer correlation. Frozen stagnation conditions behind a normal shock are calculated using Rankine–Hugoniot relations.

Spectral System

Spectral intensities were measured with a Spex Triplemate spectrometer using two different gratings. One scanned over the spectrum at a higher resolution but at a slower rate; the other scanned at a lower resolution but at a faster rate. Measured spectra were collected with a linear diode array (LDA) of 1024 diodes controlled by an optical, multichannel analyzer (OMA). The dynamic range of measurements was enhanced by a repetitive collect-and-store procedure with background subtraction. Intensities were calibrated using a tungsten ribbon filament lamp whose calibration is traceable to the National Institute of Standards and Technology.

Light from the zone of interest in the shock layer was collected by a 0.5-m focal length lens placed inside the test chamber at 0.5 m (perpendicular distance) from the flow axis. The lens axis was aligned so that it was fixed 12.7 cm from the nozzle exit. The distance of the optical axis, or sample volume, to the blunt-body surface was controlled by moving the body along the flow axis, away from or toward the nozzle exit (Fig. 1).

To limit radiation collection from the straight section of the shock layer and reduce the effects caused by shock curvature around the blunt body, a long optical path length was used. This arrangement resulted in a calculated depth of field of 8 cm for a 500-mm focal length lens using an aperture located about 8 m from the lens. This also reduced the effective radiation volume. Measurements taken with a 6-mm aperture resulted in a spatial resolution (volume diameter) of 4 mm at the arcjet flow axis and 6 mm at a distance of 6 cm from the flow axis; this resulted in a narrow-waist, pencil-shaped volume (Fig. 1, inset).

The Spex Triplemate spectrometer has a 0.6-m focal length. With this spectrometer light was detected using a 1024-element LDA detector. The higher-resolution measurements were obtained using an 1800 1/mm grating that yielded a 0.023-nm pixel resolution; the lower-resolution measurements were made with a grating of 600 1/mm and a 0.0692-nm pixel resolution. The resolution or isolated-peak full-width-at-half-maximum is 0.08 and 0.28 nm, respectively. Spectral data were recorded with an OMA. Because of the limited wavelength range subtended by the LDA, it was necessary to piece together about 20 scans at different grating settings to cover the entire range of wavelengths emitted by the N_2 (B-A) and N_2^+ (B-X) transitions. Measurements were taken at shock-layer locations separated from one another by about 6.3 mm.

Analysis Techniques

Analysis techniques for determining rotational and vibrational temperatures from measured spectra for N_2 and N_2^+, briefly summarized here for completeness, are described in Ref. 10. Most of these were developed using concepts of thermal equilibrium or Boltzmann population of rotational and vibrational states that neglect overlapping spectra of different species. Applying these techniques can yield inconclusive results if assumptions are not carefully considered. In determining vibrational state populations, overlap is considered; nothing is assumed except the Boltzmann populations of rotational states. Vibrational temperatures determined here are based on lower vibrational state populations, which tend to follow a Boltzmann trend.

While we may refer to temperatures obtained as those for N_2 or N_2^+, all analysis is based on radiation from excited electronic states of the molecules, and results basically apply to those states from which the transition originates. Under equilibrium conditions, results would apply to all states; but for some nonequilibrium cases, it is possible that each set of temperatures may be unique, not only for each molecule but for each electronic state of each molecule. Simplifying shock-layer computations requires an assumption of certain energy couplings within shock-layer flow. In the analysis made here, the general assumption is a single rotation temperature. Because determining vibrational populations depends on knowing rotational distributions, we will begin by assessing the rotational temperature.

N_2^+ Rotational Temperature from the Spectra of the (B-X) System

Techniques for determining the rotational temperature of N_2^+ are grouped into four categories. The first is the method

of ratio of intensity integrals. Spectral features, such as peaks in rotational spectrum, are integrated and ratios of integrals of calculated spectra are correlated with T_r and T_v. T_r is inferred from these correlations and from the measured ratio of integrals. Because several ratios are calculated, inferred temperatures are averaged to determine a more accurate value. Sensitivity factors are used as weighting factors in these averages to give more weight to those ratios that are more sensitive to temperature.

The second technique is the Akundi–Arepalli technique, which is a method of allocating R and P branches in the v', $v'' = 0$, 1 spectrum. Calculated or theoretical weight as a function of temperature is given to the P and R branch of each peak in the (0, 1) spectrum of the N_2^+ (B-X) transition between 424 and 428 nm. These P- and R-component-allocated intensities are plotted on a Boltzmann plot. The slope of each set of points corresponding to an assumed temperature yields a temperature that is not generally the same as the assumed temperature (Fig. 3 in Ref. 10). The correct temperature is common to the assumed temperature for the P and R branches, that is, where plots of the two temperatures cross (Fig. 4 in Ref. 10).

The third technique, called the Léger technique, is a least-squares method that minimizes the difference between measured and calculated ratios of integrals or rotational features of the (0, 1) spectrum. One may determine the best rotational temperature by using a computation algorithm or simply by plotting the rms deviation.

The fourth technique is a method that minimizes the deviation between measured and computed spectra with T_r as a parameter. This method was used simultaneously and self-consistently to determine the vibrational state populations.

N_2^+ and N_2 Vibrational Temperature

The following techniques determine the vibrational temperature from the N_2^+ (B-X) or N_2 (B-A) spectra:

1) The first technique is a least-squares fitting of basis set functions to measured spectra. A set of basis spectra for a given rotational temperature is calculated for spectral range and resolution of the experiment.[13] Each basis spectrum corresponds to a given v' level. The set of basis spectra is then fitted to the measured spectrum by adjusting the relative population of each level. If a relative population slope appears to be Boltzmann, the population slope yields the vibrational temperature. Deviation from Boltzmann populations in our cases are readily apparent, and can be seen in the higher-vibration quantum numbers. Because the N_2 (B-A) spectra overlaps with the N_2^+ (B-X) and N_2^+ (A-X) spectra, it is preferable to fit measurements to all three basis spectra simultaneously, or at least to the N_2 (B-A) and N_2^+ (A-X) spectra, which already overlap significantly. With this technique we can obtain the relative populations of vibrational energy levels of each upper electronic state. If all three basis sets are included, we can, in principle, obtain the relative populations of the N_2^+ $B^2\Sigma_u^+$ and $A^2\Pi_u$ electronic levels, thereby providing an indication of electronic temperature.

2) The second method is based on ratios of integrals of vibrational spectrum bandheads. A set of computed spectra is determined for the range of rotational and vibrational temperatures. Integrals over narrow wavelength ranges are computed, and a set of ratios of integrals is determined and plotted as functions of T_r and T_v. If we know T_r from another technique, vibrational temperatures can be inferred. Weighted averages of these inferred vibrational temperatures are determined in the same way as for rotational temperatures. This method assumes a Boltzmann distribution describes the population of vibrational states.

Results and Discussion

Spectral measurements were made in the shock layer of the rectangular blunt body in arcjet flow for conditions given in the Measurements section of this paper. Five locations in the shock layer are presented. The first, 3.5 cm from the body, was made during one sequence of measurements; and the other four were made during another sequence, about three months later. The run condition settings for the two sequences were the same; but it appears that the intensity of the two sequences differed for reasons not clearly understood, and that the shock layers may have other differences that also have not been clarified. An intensity calibration covering the optical system from end to end was made for each sequence. The measured spectra are given in Figs. 2–4, where Fig. 2 shows the higher-resolution spectrum acquired from about 320 to 480 nm; Fig. 3 shows the lower-resolution spectrum acquired in that same range; and Fig. 4 shows the lower-resolution spectrum from 500 to 800 nm.

Rotational Temperature of N_2 (B-State) and N_2^+ (A-State): Visible Spectra

The rotational temperature of N_2 alone is difficult to determine for several reasons, including the closeness of rotational lines, similar intensity distribution in the bands depending on T_r and T_v, and overlapping of the N_2 (B-A) radiation with the N_2^+ (A-X) system. Nonequilibrium effects may create problems as well because the calculation of spectra assumes Boltzmann vibrational and rotational populations. An estimate T_r for N_2 is obtained by minimizing the deviation between fitted and measured spectra. Again, fits were done for a T_r range that assumes a single rotational temperature for the two overlapping systems. The rotational temperature corresponding to the minimum rms deviation was selected as the best estimate of rotational temperature for both molecules. The vibrational state population of the B-A transition (N_2, first positive system) is determined in the fitting process, and the results are plotted in Fig. 5.

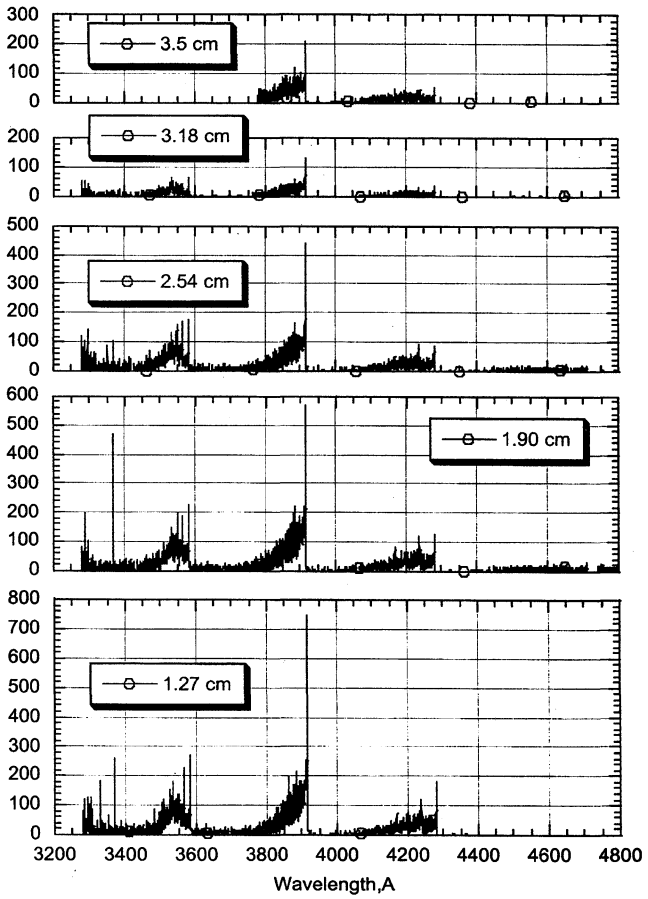

Fig. 2 Measured spectra for five locations in the blunt-body shock layer taken at a higher resolution of about 0.08 nm.

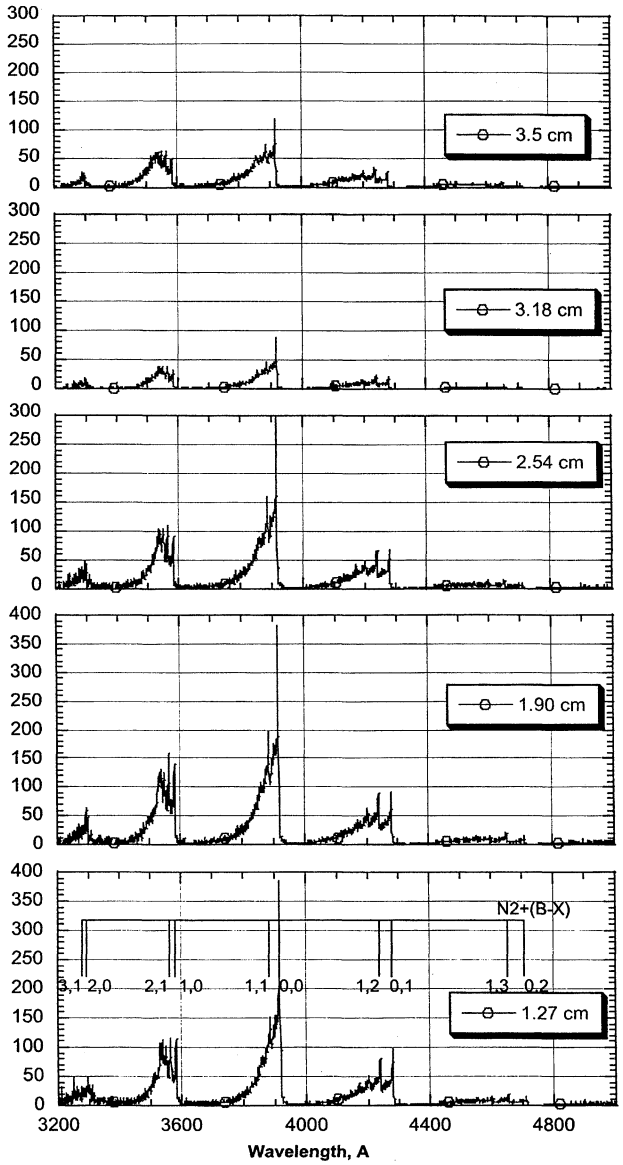

Fig. 3 Measured spectra for five locations in the blunt-body shock layer taken at a lower resolution of about 0.28 nm in the short wavelength region.

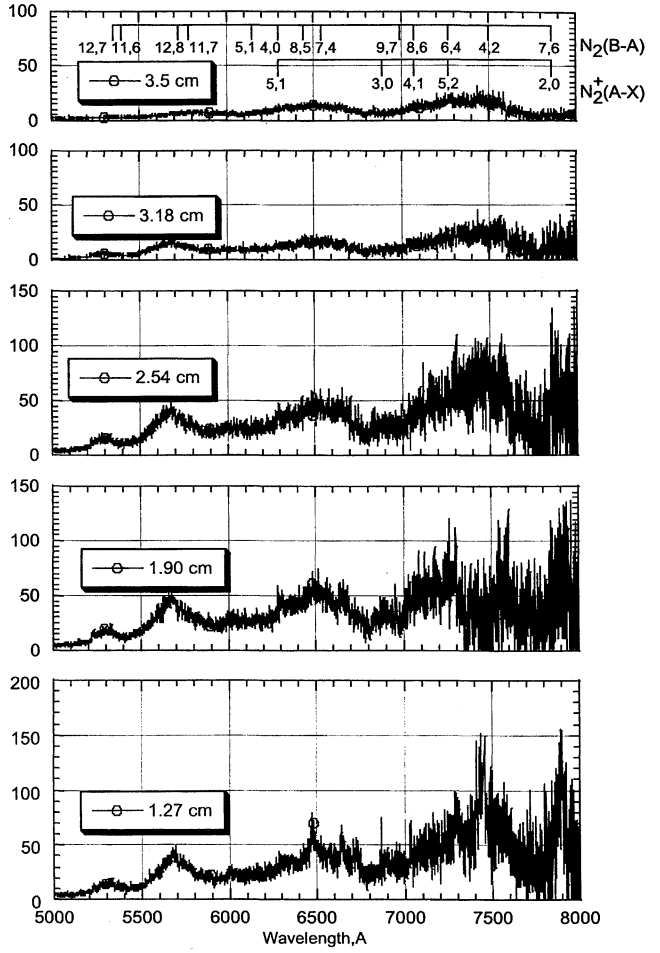

Fig. 4 Measured spectra for five locations in the blunt-body shock layer taken at a lower resolution of about 0.28 nm in the long wavelength region.

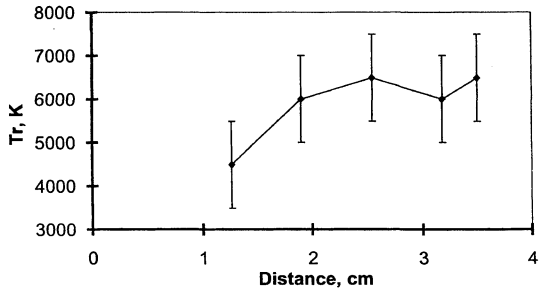

Fig. 5 Rotational temperature determined by minimizing simultaneous fits of N_2 (B-A) and N_2^+ (A-X) systems.

Rotational Temperature for N_2^+ (B-State): Ultraviolet Spectra

The rotational temperature of N_2^+ was determined using several techniques, two of which use only the (0, 1) band of the (B-X) transition. Measured ratio of intensity integrals were used to interpolate curves in which calculated ratios are plotted against T_r. Results of each ratio are averaged with one another to obtain a best estimate of temperature. The *P*- and *R*-branch allocation (Akundi–Arepalli) technique was also used to determine temperature from this band. A third technique covers several (v', v'') bands of the N_2^+ (B-X) system, minimizing the rms deviation between fitted and measured spectra. The minimum deviation here for fits of N_2^+ spectra to (B-X) basis spectra is found as T_r is varied.

The (0, 1) band of the N_2^+ (B-X) system was used to determine the rotational temperature of the B state. There is some overlap in the region because of radiation from high v' levels of the B-state $\Delta v = 2$, which may affect accurate inference of T_r, particularly if strong nonequilibrium vibrational or rotational state populations exist in the shock layer.

A summary of rotation results is given in Fig. 6, where the mean of all techniques is also shown. Approximately, these values of T_r were used to determine T_v.

Vibrational Temperature of N_2^+

Our determination of the vibrational temperature of N_2^+ was accomplished using 1) fits of N_2^+ (B-X) basis spectra to the measured spectrum from 377 to 480 nm; and 2) ratio of intensity integrals using calculated spectra from two codes that used slightly different spectral constants, the PSI code,[13] and the NEQAIR2 code.[14] Ratios of integrals took into account the background radiation described in Ref. 10. Both high- and low-resolution measurements were used. Results of the integral ratio technique are summarized in Fig. 7, where the designation "Rz" indicates that the background or zero level was subtracted before the ratios were calculated. An approximate value of T_r was assumed when calculating T_v at each distance.

Vibrational Temperature of N_2

The vibrational temperature of N_2 was determined by two techniques using the spectrum of the B-A transition (the first

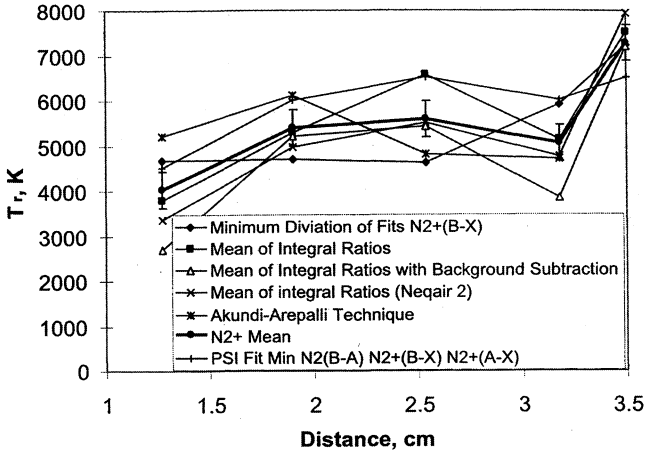

Fig. 6 Rotational temperature from various techniques with mean and estimated standard errors.

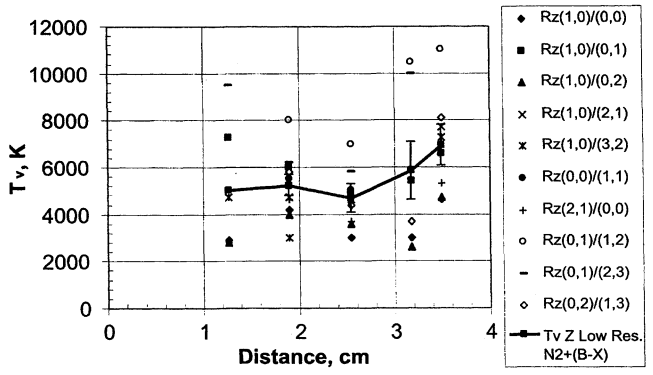

Fig. 7 Vibrational temperatures inferred from the ratio of intensity integrals for low-resolution N_2^+ (B-X) transitions. The mean is shown by a heavy solid line.

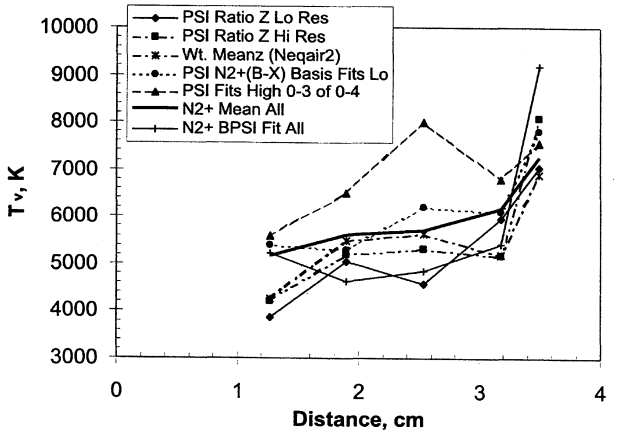

Fig. 8 Vibrational temperature from N_2^+ spectra and fits of three basis sets.

positive system) while requiring a rotational temperature input. As can be seen in Fig. 4, the spectrum presented for a 1.9-cm distance has an erroneous region between 730 and 760 nm. Similarly, the spectrum at 1.27 cm has atomic nitrogen lines that contaminate the molecular spectrum. Ratios involving these regions were therefore not used to determine temperature.

The first technique employed intensity integrals calculated from spectra using the NEQAIR2 code[14] and the PSI spectral fitting code[13] with Boltzmann-specified v' populations. These two codes used spectral constants from different sources to calculate spectra. Ranges for intensity integration are given in Ref. 10. The calculated ratios assume a Boltzmann distribution of vibrational states.

The second technique also used a PSI spectral fitting code to obtain vibrational state populations by fitting basis spectra to measured spectra. These populations were then fitted in a Boltzmann plot to yield a temperature based on the lowest four or five levels. Although the first few levels of Boltzmann plots described a good, straight line, the higher v' state populations deviated from Boltzmann.

In Fig. 8, the averages of all vibrational techniques are compared. Most of these cluster together, except the one for the higher-resolution basis set fit technique, which yields somewhat higher results. This may be because only four or five levels are used in a fit that covered up to 21 levels. Only the bandheads involving lower states can be used reliably because of possible overpopulation in the higher states.

Because the N_2 (B-A) radiation is overlapped by the N_2^+ (A-X) system, spectral fits for this wavelength region should employ both systems, although a near fit may be obtained using only the first positive system. The overlapping N_2^+ (A-X) spectrum is relatively weak but not negligible, and there is too much uncertainty in the A-state populations obtained from the fits to derive a Boltzmann temperature. Results can differ when different wavelength intervals for a fit are used. For example, the PSI code ignores the N_2^+ (A-X) altogether if wavelengths covering the first transition from the $v' = 2$ state are not included. Overlap in basis spectra tends to produce errors in populations determined by the code, with possible uncertainties in higher v' populations so large that a finite positive population for certain levels may not be produced at all. In such cases, the code sets the population to zero. While it is convenient to be able to determine populations and temperatures from particular wavelength intervals in the spectra, we adapted the PSI code to handle three systems simultaneously over much of the spectrum. This was done to avoid errors caused from the range and overpopulation of higher states and state population cutoffs, and to provide a means of checking temperatures derived separately from various spectral ranges.

Vibrational Populations of the N_2 B, N_2^+ B, and N_2^+ A States

By using the PSI code spectral-fitting technique, we simultaneously determined the relative populations of the N_2 B, N_2^+ B, and N_2^+ A states. As before, low v' state populations seem to follow a Boltzmann distribution, but the upper v' levels do not. Only one distribution, the first positive system that measured 3.5 cm from the surface, showed Boltzmann behavior up to $v' = 17$. This is the measurement farthest from the body, and it comes from a different sequence of measurements. Resultant populations of the N_2^+ B state for $v' = 0$–17 are shown in Fig. 9, the resulting N_2^+ A-state populations of the $v' = 2$–21 states are shown in Fig. 10, and the N_2 B state appears in Fig. 11. The v' levels for the N_2 B and N_2^+ A states start at

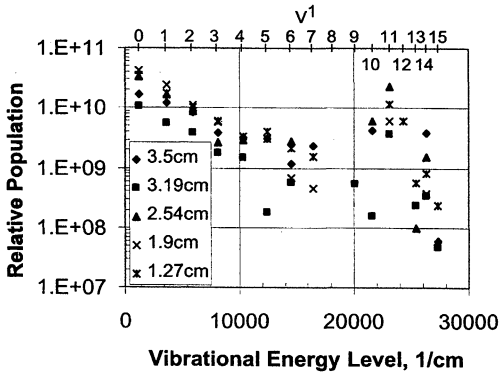

Fig. 9 Population of the N_2^+ B state in a shock layer at different distances from the body.

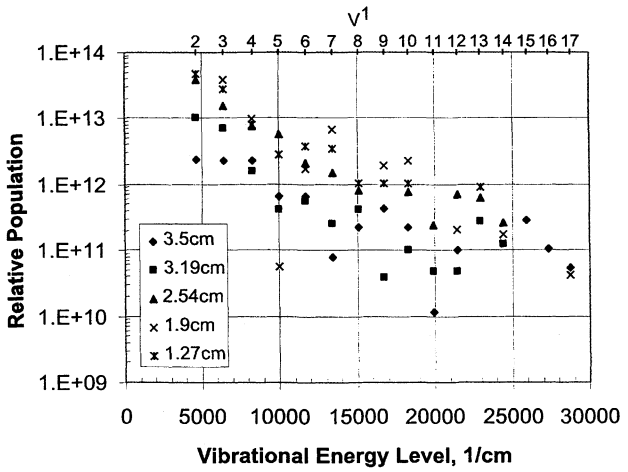

Fig. 10 Population of the N_2^+ A state in a shock layer at different distances from the body.

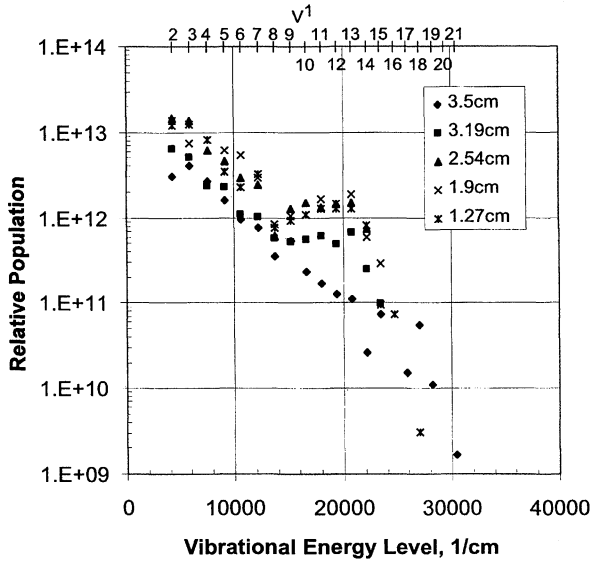

Fig. 11 Population of the N_2 B state in a shock layer at different distances from the body.

2 because emission from $v' = 0$ and 1 is outside the spectral measurements range.

The plots of Figs. 9–11 indicate that the lower v' levels tend to follow a straight line (Boltzmann behavior); however, at energies above about 12,000–15,000 cm, the populations tend to be greater than those based on a Boltzmann population at a temperature corresponding to the first few levels.[14] Such a trend has been observed in electrical discharges of nitrogen and CO.[15–17] These are believed to be the first vibrational population measurements made in the shock layer of an arcjet flow. The opposite trend (populations lower than a Boltzmann distribution) has been predicted for shock layers where the freestream is undissociated and its velocity is high.[18] The behavior observed in Figs. 9–11 may be related to the fact that the freestream in arcjets is significantly dissociated and probably partially ionized, with electrons frozen at a relatively high temperature.

To be certain that overpopulation of the upper vibrational states was not a result of code-fitting errors or problems with wavelength range, fits were attempted using Boltzmann populations of the basis sets at or near the temperatures found. These did not agree well with measurements and are particularly noticeable in the wavelength ranging from about 500 to 600 nm. At various temperatures the qualitative comparison of spectra shows the same behavior for all but the first position

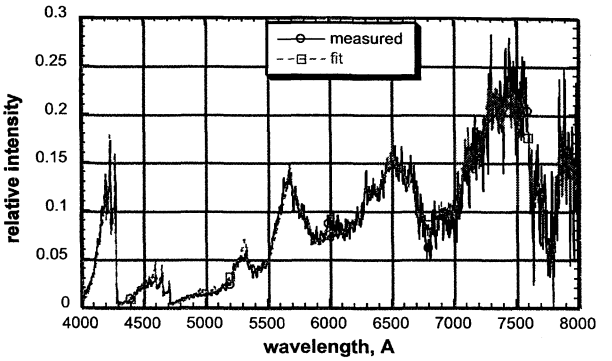

Fig. 12 Comparison of measured spectrum, at a distance of 2.54 cm, with that computed by fit to three basis sets, N_2 (B-A), N_2^+ (B-X), and N_2^+ (A-X).

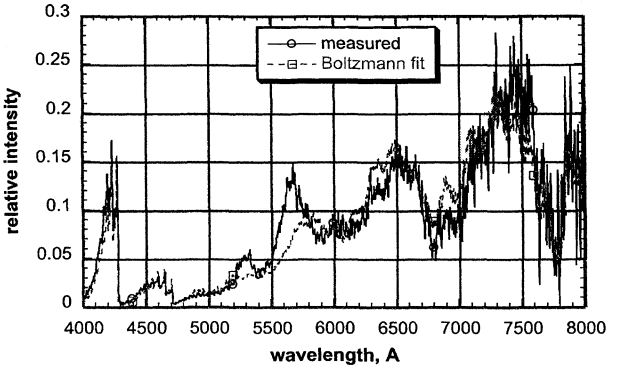

Fig. 13 Comparison of measured spectrum, at a distance of 2.54 cm, with that calculated assuming a Boltzmann population of N_2 (B-A) at T_r = 7500 K and T_v = 7000 K, and N_2^+ (B-X) and N_2^+ (A-X) at T_r = 5000 K and T_v = 5500 K.

(3.5 cm). For example, in the spectrum taken at 2.54 cm from the surface (Fig. 12), the measured spectrum is compared with the spectral fit that incorporated vibrational basis sets from N_2 (B-A), N_2^+ (B-X), and N_2^+ (A-X) electronic transitions. The fitted spectrum matches the measurements well over the whole wavelength range; but the agreement is not as good if we assume Boltzmann populations. In Fig. 13, the measured spectrum is compared with a spectrum calculated assuming Boltzmann populations of states including N_2 (B-A) at T_r = 7500 K and T_v = 7000 K, and N_2^+ (B-X) and N_2^+ (A-X) at T_r = 5000 K and T_v = 6500 K. This temperature combination seemed to yield the best overall agreement of measured and calculated spectra after we tried many combinations. The spectra still deviate considerably in the spectral range of 500–600 nm; however, there is also some deviation at other wavelengths. Nor can the deviation be explained by overlapping of the N_2^+ (A-X) spectrum.

Comparisons of N_2 and N_2^+ Temperatures and Populations

The vibrational and rotational temperatures for N_2 and N_2^+ based on lower vibrational levels are shown in Fig. 14, where it can be seen that the temperatures differ significantly at the farthest two points from the body. This difference is greater than the standard error (estimated to be about 300 K). It is not clear why this temperature difference occurs between the two species. Although a detailed interpretation of this finding is outside the scope of this paper, some possibilities are discussed herein.

A principal reason for the lack of a more complete analysis is our lack of knowledge about the state of the gas upstream of the shock. The freestream in arcjets proceeds from the nozzle expansion of a uniform arc-heated gas, thus making it difficult to establish local enthalpy. However, in our case local enthalpy could be as high as three times bulk enthalpy. And,

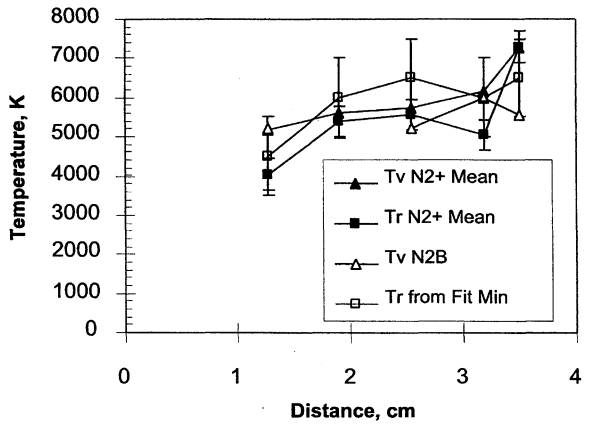

Fig. 14 Vibrational and rotational temperature distributions in a shock layer.

at three times bulk enthalpy the reservoir temperature would be about 6100 K. This temperature range should establish bounds on the vibrational energy in the freestream; and it is likely that the freestream vibrational temperature is about half the stagnation temperature because of relaxation in the expansion.[19] The energy distribution and excitation of nitrogen molecules in the freestream is, in fact, unknown. The peak in population distribution at $v' = 3$ for the N_2 B state found at the position nearest the shock front (at 3.5 cm) would indicate that distribution was likely formed by excitation from a ground state strongly populated at the $v = 0$ level, possibly reflecting the freestream distribution and resultant temperature.[20] That is no longer the case as the flow moves toward the body, where the ground and excited state populations are influenced by higher temperature conditions in the shock layer.

As the flow approaches the body, the spectrum associated with the (B-A) transition of N_2 has a peaked behavior in the region of 500–600 nm, which is a consequence of overpopulation in higher vibrational states. It is possible that the atoms recombine to form N_2 in highly excited states,[21–23] particularly leading to an overpopulation of v' states 10–14. This may result in a higher vibrational temperature.

Formation of N_2^+ as flow approaches the body is probably a result of associative ionization

$$N + N \rightarrow N_2^+ + e$$

or possibly a result of the direct impact of hot electronics that originate in the arc and stay frozen at high energies

$$e + N \rightarrow e + e + N^+$$

followed by the charge exchange

$$N^+ + N_2 \rightarrow N_2^+ + N$$

The B state of the ion shows an overpopulation of upper states at 3.5 cm, which the neutral molecule does not. The evolution of excited atomic nitrogen is unclear from the data. Radiation from nitrogen atoms is observed at 1.27 cm, but is not seen farther from the body. It would appear that a sharp increase in N-atom density occurs well into the shock layer near 1.27 cm.

The rotational temperatures are close to the corresponding vibrational temperatures for N_2 and N_2^+, respectively. This may be fortuitous because of the 1000 K uncertainty in the assessment of rotational temperature for N_2.

Conclusions

Spectral measurements in the shock layer of a blunt body in an arcjet flow have been analyzed to estimate rotational and vibrational temperatures from several techniques, and to determine vibrational state populations of the N_2 B, N_2^+ B, and N_2^+ A-states. It was found that the populations of a few lower states tend to follow a Boltzmann distribution from which vibrational temperatures were determined; but higher states deviate significantly from equilibrium. The overpopulation of certain N_2 B-v' states significantly affects the character of the spectrum in the wavelength range 500–650 nm.

From these first measurements of vibrational populations in an arcjet shock layer, we found that low-density arcjets produce nonequilibrium populations of vibrational states. This overpopulation of upper vibrational states can lead to significant errors in determining temperature. We also found that much care must be used to avoid erroneous temperature results from using ratio and fitting techniques because upper states contribute radiation not at just one wavelength region but throughout the spectrum. The N_2^+ (B-X) system, for example, may contribute weak radiation into the long wavelength region through 800 nm, a negligible amount if upper-state populations follow a Boltzmann distribution. But, if overpopulated upper states are left out when attempting to fit the spectra here, the fit may result in erroneously high populations of the lower states, leading to somewhat different vibrational temperatures.

In some cases temperatures determined from different techniques differed more than expected (Fig. 8). While the techniques for determining temperature are generally reliable, care must be exercised in their use, particularly when evaluating spectra from a highly nonequilibrium high-temperature source. For example, a simple technique developed to determine vibrational temperatures of N_2 from ratios of Δv-interval intensities from the first positive system (B-A) can yield accurate results if the radiation in the 500–800 nm region is only from the first positive system and if there is a Boltzmann population. In the shock layer here, substantial radiation from the molecular nitrogen ion, N_2^+ (A-X), invalidates a temperature assessment of N_2 by that method. Because the results indicate non-Boltzmann behavior and because of overlapping systems, the ratio technique could not be used to determine T_v for N_2.

In cases where a technique for determining the vibrational temperature depends on a rotational temperature, an error in rotational temperature contributes to an error in vibrational temperature. Also, an error in fitting technique may result from excluding vibrational states in the fitting process or a lack of wavelength alignment of measured and theoretical spectra. Temperature results may also be somewhat dependent on the wavelength range used in the fit, whereas differences in temperature obtained by different methods may result from large statistical uncertainties,[10] much of the error stems from nonequilibrium. Even when the three radiative systems are used together in a total fit, it is difficult to obtain accurate populations for the upper states because of overlapping spectra. Indeed, all three systems overlap strongly in the midwavelength region.

The upper state populations obtained nevertheless show a trend away from a Boltzmann distribution, and there are some indications that differences in temperature could exist even between the A and B states of N_2^+. It is certain that electronic temperatures differ.

Development of the state to state vibrational exchange approximations has allowed flow code computations without requiring a Boltzmann population of electronic states. In recent years work was done to develop models that handle non-Boltzmann vibrational populations and to understand the effects of this distribution on thermodynamic properties. Ultimately, a multitemperature gas kinetic model for N_2^+ and N_2 that includes vibrational state nonequilibrium will be required. Measurements such as those presented here may provide the basis for validating such a model.

Acknowledgments

Thanks are extended to Eric Yuen for help with data collection, and to William Marinelli of Physical Sciences, Inc., for

furnishing the spectral fitting code. The authors are indebted to Christophe Laux for furnishing certain spectral constants and the NEQAIR2 code.

References

[1]Allen, R. A., "Nonequilibrium Shock Front Rotational, Vibrational, and Electronic Temperature Measurements," AVCO-Everett Research Rept. 186, Everett, MA, Aug. 1964.

[2]Blackwell, H. E., Wierum, F. A., Arepalli, S., and Scott, C. D., "Vibrational Temperature Measurements of N_2 and N_2^+ Shock Layer Radiation," AIAA Paper 89-0248, Jan. 1989.

[3]Blackwell, H. E., Yuen, E., Arepalli, S., and Scott, C. D., "Nonequilibrium Shock Layer Profiles from Arc Jet Radiation Measurements," AIAA Paper 89-1679, June 1989.

[4]Blackwell, H. E., Arepalli, S., Yuen, E., and Scott, C. D., "Analysis of N_2 Shock Layer Emission and the Measurements of Arc Jet Temperatures," AIAA Paper 90-1736, June 1990.

[5]Blackwell, H. E., Wierum, F. A., and Scott, C. D., "Spectral Determination of Nitrogen Vibrational Temperatures," AIAA Paper 87-1532, June 1987.

[6]Blackwell, H. E., and Scott, C. D., "Measured Rotational and Vibrational Temperature Differences in Arc Jet Shock Layers," AIAA Paper 92-3030, June 1992.

[7]Akundi, M. A., "LIF and Emission Studies of Copper and Nitrogen," NASA/ASEE Summer Faculty Fellowship Program, NASA Johnson Space Center, Aug. 1990.

[8]Winter, M. W., Auweter-Kurtz, M., and Kurtz, H. L., "Investigation of an Equilibrium Condition Boundary Layer in Front of a Material Probe in a Subsonic Plasma Flow," AIAA Paper 96-1853, June 1996.

[9]Park, C. S., Newfield, M. E., Fletcher, D. G., Gökçen, T., and Sharma, S. P., "Spectroscopic Emission Measurements Within the Blunt-Body Shock Layer in an Arc-Jet Flow," AIAA Paper 97-0990, Jan. 1997.

[10]Scott, C. D., Blackwell, H. E., Arepalli, S., and Akundi, M. A., "Techniques for Determining Rotational and Vibrational Temperatures in Nitrogen Arc Jet Flow," AIAA Paper 97-2521, June 1997; also "Techniques for Estimating Rotational and Vibrational Temperature in Nitrogen Arcjet Flow," *Journal of Thermophysics and Heat Transfer*, Vol. 12, No. 4, 1998, pp. 457–464.

[11]Bouslog, S. A., Caram, J. M., and Pham, V. T., "Catalytic Characteristics of Shuttle High-Temperature TPS Materials," AIAA Paper 96-0610, Jan. 1996.

[12]Bade, W. L., and Yos, J. M., "The NATA Code—Theory and Analysis," NASA CR-2547, June 1975.

[13]Piper, L. G., Marinelli, W. J., Rawlins, W. T., and Green, B. D., "The Excitation of IF($B^3\Sigma_{u+}$) by $N_2(A^3\Sigma_u^+)$," *Journal of Chemical Physics*, Vol. 83, No. 11, 1985, pp. 5602–5609.

[14]Laux, C. O., "Modeling the UV and VUV Radiative Emission of High Temperature Air," AIAA Paper 93-2802, July 1993.

[15]Piper, L. G., and Marinelli, W. J., "Determination of Non-Boltzmann Vibrational Distributions of $N_2(X, v'')$ in He/N_2 Microwave Discharge Afterglow," *Journal of Chemical Physics*, Vol. 89, No. 5, 1988, pp. 2918–2924.

[16]Cacciatore, M., Capitelli, M., and Gorse, C., "Nonequilibrium Dissociation and Ionization of Nitrogen in Electrical Discharges: The Role of Electronic Collisions from Vibrationally Excited Molecules," *Chemical Physics*, Vol. 66, Nos. 1 and 2, 1982, pp. 141–151.

[17]Brechignac, P., Martin, J. P., and Taieb, G., "Small-Signal Gain Measurements and Vibrational Distribution in CO," *IEEE Journal of Quantum Electronics*, Vol. QE-10, No. 10, 1974, pp. 797–802.

[18]Gonzales, D. A., and Varghese, P. L., "A Simple Model for State-Specific Diatomic Dissociation," *Journal of Physical Chemistry*, Vol. 97, No. 9, 1993, pp. 7612–7622.

[19]Park, C., and Lee, S.-H., "Validation of Multitemperature Nozzle Flow Code," *Journal of Thermophysics and Heat Transfer*, Vol. 9, No. 1, 1995, pp. 9–16.

[20]Morrill, J., and Benesch, W., "Plasma Preconditioning and the Role of Elevated Vibrational Temperature in Production of Excited N_2 Vibrational Distributions," *Journal of Geophysical Research*, Vol. 95, No. A6, 1990, pp. 7711–7724.

[21]Gessman, R. J., Laux, C. O., and Kruger, C. H., "Experimental Study of Kinetic Mechanisms of Recombining Atmospheric Pressure Air Plasma," AIAA Paper 97-2364, June 1997.

[22]Laux, C. O., Gessman, R. J., and Kruger, C. H., "Mechanisms of Ionizational Nonequilibrium in Air and Nitrogen Plasmas," AIAA Paper 95-1989, June 1995.

[23]Partridge, H., Langhoff, S. R., and Bauschlicher, C. W., "Theoretical Study of $A'^5\Sigma_g^+$ and $C'^5\Pi_u$ States of N_2: Implications for the N_2 Afterglow," *Journal of Chemical Physics*, Vol. 88, No. 5, 1988, pp. 3174–3184.